JOURNAL OF GEOPHYSICAL RESEARCH, SPACE PHYSICS VOL. 73, NO. 9, MAY 1, 1968

Ducted Whistler-Mode Propagation in the Magnetosphere; A Half-Gyrofrequency Upper Intensity Cutoff and Some Associated Wave Growth Phenomena

D. L. CARPENTER

Radioscience Laboratory, Stanford University
Stanford, California 94035

A large class of ducted magnetospheric whistlers exhibits an upper intensity cutoff at which the wave amplitude decreases by >10 db within a fraction of a kHz. A preliminary study, based in large part on whistlers recorded at Eights, Antarctica ($L \sim 4$), indicates that the ratio of cutoff frequency to whistler nose frequency f_{co}/f_n is invariant with respect to path equatorial radius, local time, and magnetic activity. Measurements on 541 whistler components propagating in the plasmasphere were such that $f_{co}/f_n = 1.33 \pm 0.08$ for about 70% of the cases. The corresponding result for f_{co}/f_{H_0}, the ratio of cutoff frequency to minimum path gyrofrequency, is $f_{co}/f_{H_0} = 0.51 \pm 0.03$. (To relate f_n and f_{H_0}, the approximate relation $f_n = 0.38 f_{H_0}$ was used, from Angerami's work on the diffusive-equilibrium model of the distribution of thermal ionization along the field lines in the plasmasphere.) The observed behavior of f_{co}/f_{H_0} is apparently controlled by a propagation effect and not by a resonant particle damping process, the propagation effect probably being the half-gyrofrequency upper limit on ducted whistler-mode propagation in tubes of enhanced ionization predicted by Smith. Spectrographic VLF records exhibit much evidence of wave growth in the 0.4–0.5 f_{H_0} band, an example being the stimulation of noise at $\sim$0.5 f_{H_0} by both whistlers and a low-power ($\sim$100 watts) controlled source. A whistler-triggering event may include: an intensity maximum above the whistler nose, followed by a slight dispersion anomaly and the cutoff; a quasi-constant triggered noise tone with bandwidth <100 Hz, duration ranging from $\sim$30 msec to >1 sec, and intensity comparable to that of the associated whistler. The noise tone itself does not usually exhibit dispersive whistler-mode echoing, nor does it exhibit an intensity cutoff as it rises in frequency through the 0.5 f_{H_0} level. Earlier observations by Kimura of triggering of magnetospheric noise by $\sim$1-sec, 10.2-kHz pulses from the Omega transmitter at Forest Port, New York, have been extended to show that the triggering is confined in space to a range of paths with minimum gyrofrequency within a few per cent of twice the transmitted frequency. A similar tendency is evident in noise produced by high-power ($\sim 10^6$ watts) transmitters. A crude ampligram analysis of the cutoff effect shows that in a typical example the whistler wave intensity drops roughly 20 db within a time interval <13 msec and a frequency interval <50 Hz.

INTRODUCTION

The fact that many natural whistlers exhibit well-defined, broadband characteristics invites attention to the use of whistler spectra in studies of the nature of wave-particle interactions in the magnetosphere of the earth. In particular, one might hope to examine the amplitude spectrum of whistlers and, from an appropriate theory of the interaction process, deduce important characteristics of the velocity and pitch-angle spectra of magnetospheric electrons in the kev range.

The first attempt of this kind was made by *Scarf* [1962], who drew attention to an abrupt upper cutoff effect in which the whistler wave intensity drops on the order of 10 db within a fraction of a kHz. This effect is illustrated in Figure 1 (see Plate 1, page 2932) by several multi-component whistlers recorded at Eights, Antarctica ($L \sim 4$), during 1963. The coordinates are frequency in kHz and time in seconds from the initiating atmospheric. In *Scarf*'s [1962] work and in several other papers, experimental information on the whistler cutoff was combined with models of a cyclotron resonance interaction in the magnetosphere to yield information on the particles taking part in the damping process [see, for example, *Liemohn and Scarf*, 1962*a*, *b*, 1964; *Guthart*, 1965*a*]. Also investigated were thermal effects on the frequency-versus-time, or dispersion, properties of a whistler in the vicinity of the cutoff frequency [*Guthart*, 1965*b*]. *Liemohn* [1967] recently made calculations relating the amplitude spectrum of an observed whistler to both the velocity and pitch-angle spectra of the resonant magnetospheric electrons.

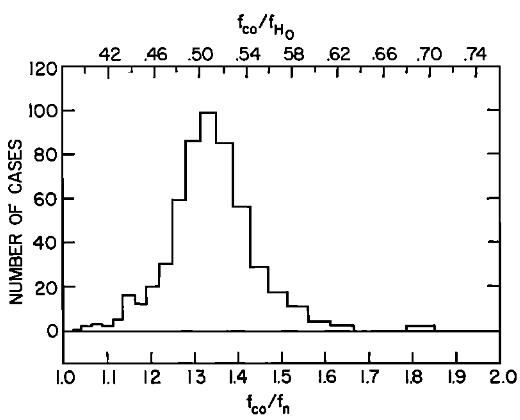

Fig. 2. Distribution of observed values of the ratio of whistler cutoff frequency to nose frequency, f_{co}/f_n. 541 whistler traces were measured, most of them having been recorded in June–August 1963 at Eights, Antarctica ($L \sim 4$). The relation between f_{co}/f_n and the scale for f_{co}/f_{H_0} (top) is based on calculations of the ratio f_n/f_{H_0} by *Angerami* [1966].

Experimental work on the intensity-versus-frequency properties of whistlers has been meager by comparison with the scope of theoretical activity. There are now plenty of good experimental data, and the imbalance may be corrected.

The present paper is concerned with upper cutoff effects that typically involve a drop in wave amplitude of 10 db or more in $\Delta f < 100$ Hz. Such effects are characteristic of paths with equatorial radii $> 3.5\ R_E$. (The lower rate of occurrence on paths with shorter radii may be due to a falloff above 10 kHz in the amplitude spectrum of whistler lightning sources.) It is found that to a first approximation, the upper cutoff occurs at a fixed value of the ratio of wave frequency to minimum path gyrofrequency f_{co}/f_{H_0}, regardless of variations in local time, path equatorial radius, or magnetic activity. This fixed value of f_{co}/f_{H_0} is $\sim$0.5 (determined from the observations and from calculations employing a diffusive-equilibrium model of the field-line distribution of electrons [*Angerami*, 1966]). There is evidence of whistler wave growth in the subcutoff range $\sim 0.4\ f_{H_0} < f \leq 0.5\ f_{H_0}$, one effect being the anomalous half-gyrofrequency triggering of magnetospheric noise by fixed-frequency 10.2-kHz signals from a low-power ($\sim$100 watts) transmitter.

Two mechanisms for an upper cutoff have been advanced, one involving a cyclotron resonance interaction [e.g., *Liemohn*, 1967], and the other a propagation effect, wherein 0.5 f_H (f_H = local gyrofrequency) is predicted as a natural upper limit to the trapping of whistlers in field-aligned columns of enhanced ionization [*Smith*, 1961]. The results of the present paper do not support one or the other mechanism unambiguously; however, the weight of the evidence suggests that the trapping theory may explain the 0.5 f_{H_0} value of f_{co}, whereas an interaction process must be considered to explain the wave amplitude phenomena occuring just at and below 0.5 f_{H_0}.

The present paper contains three main sections, one on the statistics of the upper cutoff frequency, a second on wave growth and noise phenomena, and a third on whistler and noise amplitude spectra near the cutoff.

Experimental Results on the Cutoff Frequency

In this section are reported statistics on the ratio of whistler upper cutoff frequency to nose frequency, f_{co}/f_n (f_n = frequency of minimum travel time). Most of the data were taken from 1963 austral-winter recordings at Eights, Antarctica, supplemented by measurements on the USNS *Eltanin* research ship and at Byrd Station, Antarctica. The analysis involved preparation of 35-mm films on the Rayspan spectrum analyzer and frequency scaling, using a digitizing x–y plotter. Records exhibiting well-defined events with peak intensities 20 db or more above the

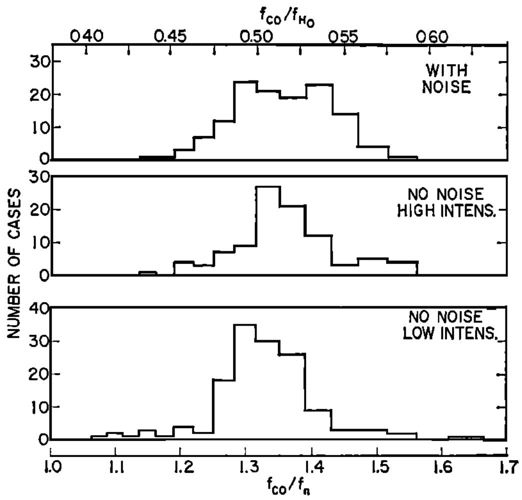

Fig. 3. Some effects of the presence of noise triggered at or near the intensity cutoff on the distribution of observed values of the ratio of whistler cutoff frequency to nose frequency.

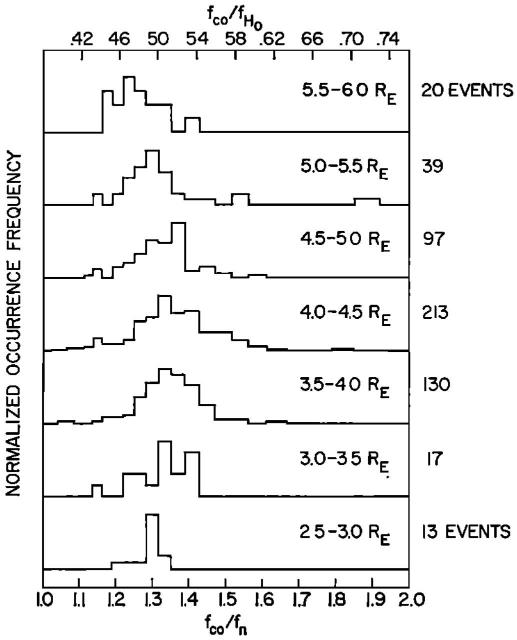

Fig. 4. Effect of variation in whistler path equatorial radius on the distribution of observed values of the ratio of whistler cutoff frequency to nose frequency.

background noise were selected to place maximum emphasis on magnetospheric propagation factors as opposed to factors such as the amplitude spectrum of the lightning source and subionospheric propagation conditions.

For the region inside the plasmapause, 541 measurements of the upper cutoff and nose frequency were made on whistlers representing 65 synoptic or continuous recording periods on 25 days. For each measured whistler component, crude visual information was taken on the intensity variation at the cutoff and on the presence of triggered noise. In most cases, the cutoff frequency could be scaled with a precision of 2% or better and the nose frequency with a precision of about 2%.

A histogram for all 541 values of the ratio f_{co}/f_n is shown in Figure 2. At the top is a derived scale for f_{co}/f_{H_0}, the ratio of cutoff to minimum path gyrofrequency (see later explanation of this scale). The data are divided into intervals of the order of 2.5% of the ratio values, a percentage comparable to the uncertainty associated with the measurements. The distribution is strongly peaked at $\sim f_{co}/f_n = 1.33$, or $f_{co}/f_{H_0} = 0.51$. Approximately 75% of the cases above the peak are below $f_{co}/f_{H_0} = 0.54$; 68% below the peak are above $f_{co}/f_{H_0} = 0.48$. Roughly one-third of the spread in the data can be explained by the mixing of cases both with and without noise tones initiated at or near the cutoff. Examples of such noise tones are shown in Figure 1. The effect on the statistics is illustrated in Figure 3, where separate histograms are plotted for: (1) whistlers with noise triggered at the cutoff (top); (2) whistlers with high intensity near the cutoff ($\sim$20–30 db above background) but free of triggering (middle); (3) whistlers with low intensity near the cutoff ($\sim$10–20 db above background) and free of triggering. It is clear that cases with noise contributed disproportionately to the right side of the composite histogram of Figure 2.

The data illustrated in Figure 2 were sufficiently distributed with respect to local time, path equatorial radius, and magnetic and solar conditions to suggest that variations in these quantities do not strongly affect the ratio f_{co}/f_{H_0}. Histograms showing the frequency of occurrence of various values of f_{co}/f_n as a function of equatorial crossing of the field line path (in a dipole geometry) are shown in Figure 4.

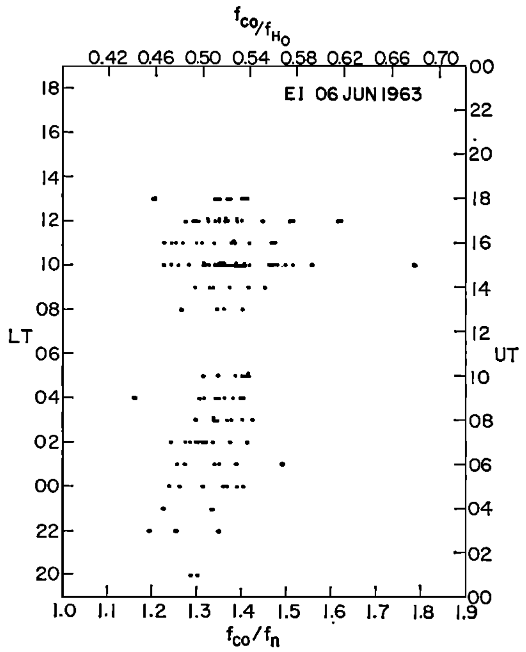

Fig. 6. Diurnal variation of observations of the ratio of cutoff frequency to nose frequency for a single day of very low magnetic activity ($Kp \sim 0$).

The 90% width of the distributions is roughly constant, and the median values of f_{co}/f_{H_0} are ~0.51 over the range 3.0–5.0 R_E and only a few per cent less outside this range. The small variations in the figure are probably not interpretable with the amount of data that has thus far been scaled. An example of the cutoff occurring at a roughly constant ratio of f_{co}/f_n over the range $L \sim$ 3–5.5, is shown in Figure 5, upper panel (see Plate 2, page 2933).

Local-time variations in measured f_{co}/f_n are illustrated in Figure 6, which shows Eights data from a day of very low magnetic activity ($Kp \sim 0$). Between 0000 and 1300 LT, the hourly median values remain within ~±2% of 1.33 (f_{co}/f_{H_0} = 0.51). In the 1000–1200 LT period there are several relatively high individual values, probably associated with the morning peak in both whistler and noise activity [e.g., *Laaspere et al.*, 1963, 1964; *Helliwell*, 1965].

Most of the data of Figure 2 represent relatively quiet magnetic conditions, with Kp in the range 0–3. Within this range there is no apparent magnetic effect. A visual examination of several hundred records for Kp = 3–6 failed to reveal disturbance-associated shifts in the cutoff. The same is true for solar cycle effects, none having been detected in a visual examination covering 1959–1967.

Evidence of Wave Growth near 0.5 f_{H_0}

There is clear evidence of amplification of whistler waves in the magnetosphere. Some important indications of this effect were recently discussed by *Liemohn* [1967]. The evidence of whistler wave growth occurs both in the amplitude spectra of whistlers and certain VLF emissions and in properties of magnetospheric noise triggered by whistler-mode signals. For both the amplitude spectra and triggered noise, the geomagnetic field appears to be a controlling factor, and wave growth phenomena present a relatively fixed pattern when plotted in normalized frequency, f/f_{H_0}. Examples of this are shown by two Eights records in Figure 7 (see Plate 2, page 2933). The upper spectrum shows a multicomponent whistler with a particularly intense cluster of traces at t = 2.2 sec. This intense group, with nose frequency $f_n \sim$ 4.5 kHz, is followed at t = 6.6 sec and t = 11.0 sec by third-hop and fifth-hop echoes. Between successive echoes at least 9 separate periodic emission elements are evident, each with a 2-hop spacing approximately equal to that between the whistler echoes. The emission activity is limited in bandwidth to approximately the 0.4–0.5 f_{H_0} range. This is a characteristic of many discrete periodic emissions; often they are restricted to still narrower ranges near 0.5 f_{H_0}. (The phenomenon of periodic emissions has been described by *Brice* [1965] and *Helliwell* [1965].)

The lower spectrum of Figure 7 shows another type of intense activity on a single path (or narrow range of paths). In this case the whistler rate on the path with nose frequency $f_n \sim$ 3 kHz is as high as the background atmospheric rate, an uncommon occurrence that suggests amplification of signals from many weak (and normally nonwhistler-producing) sources. The abrupt 0.5 f_{H_0} cutoff of the traces at ~4 kHz produces a banded effect. Many of the traces show a peak intensity near the cutoff, and the whistler with origin at $t \sim$ 4.0 sec and first hop at $t \sim$ 6.0 sec exhibits a noisy third-hop component near the cutoff frequency at $t \sim$ 10.0 sec.

Some of the strongest evidence of wave growth near 0.5 f_{H_0} comes from natural and controlled-source triggering at the cutoff frequency. (A brief description of triggering by natural whistlers is given in the next section.) Triggering of noise by fixed-frequency VLF transmitters has been investigated in recent years [*Helliwell et al.*, 1964; *Helliwell*, 1965], and it now appears that much of the triggering, particularly that produced by low-power transmitters, is a 0.5 f_{H_0} effect. In a recent study of 1963 Eights records, *Kimura* [1968] found four cases of triggering of noise in the magnetosphere by low-power, ~100 watt transmissions from the Omega transmitter at Forest Port, New York. The paths were found to cross the equator in the range 3.5–3.7 R_E, where f_{H_0} is roughly twice the transmitter frequency of 10.2 kHz. Omega triggering was examined in further detail for purposes of the present study. An example of an event is shown in Figure 8 (see Plate 3, page 2934), where three Eights spectra from a single 2-minute run are aligned in time with spectra recorded simultaneously in the conjugate hemisphere at Great Whale (GW). On the upper Great Whale record the ~1-sec Omega transmissions from Forest Port, New York; Haiku, Hawaii; and Balboa, Canal Zone, are identified as FP, H, and B, respectively. Beneath each GW panel, the

Forest Port signals are drawn with a time delay Δ = 1.35 sec from the time of observation at Great Whale. These delayed signals are to be compared with the actual received pulses at Eights on the spectra just below. The agreement in time appears to be within a few per cent of Δ, and it is inferred that, although there may be faint evidence of direct subionospheric propagation from the Canal Zone transmitter near 0651:51, the Forest Port signals are detected only after propagation in the whistler mode. The absence of time spreading of the received pulses suggests a narrow range of magnetospheric paths. On the top EI panel, both of the successive Forest Port signals show irregular intensity and frequency fluctuations. On the middle and bottom panels, representing conditions about 1 minute later, alternate Forest Port signals are anomalously intense and give rise to well-defined noise tones. The bandwidth of the intense part of the signals is $\sim\pm75$ Hz around 10.2 kHz. The rise in intensity to an anomalously high level appears to require about $\sim$100 msec for these 2 pulses.

The magnetic shell of the path or range of paths on which the Omega triggering occurred may be estimated by identifying the whistler path for which the travel time is 1.35 sec at 10.2 kHz. This interval is laid off from the causative atmospheric of an EI whistler in the upper panel of Figure 8. At 10.2 kHz, it terminates near the leading edge of a group of traces with f_{co} near the Omega frequency. The results for this case and others in the first group of Omega events to be identified are presented in Figure 9, where horizontal bars show for individual 2-minute runs the estimated range of possible values of the ratio $10.2 \times 10^3/f_{H_0}$. In several cases, the more probable region is indicated by the heavy part of the line. Below the Omega results is a flag summarizing the behavior of whistlers with noise stimulated at or near the cutoff (cf. Figure 3, top). For the Omega triggering, just as for the whistler-triggered noise, a strong $\sim0.5\ f_{H_0}$ tendency is evident.

Triggering by high-power transmitters radiating 10^5–10^6 watts has been observed throughout

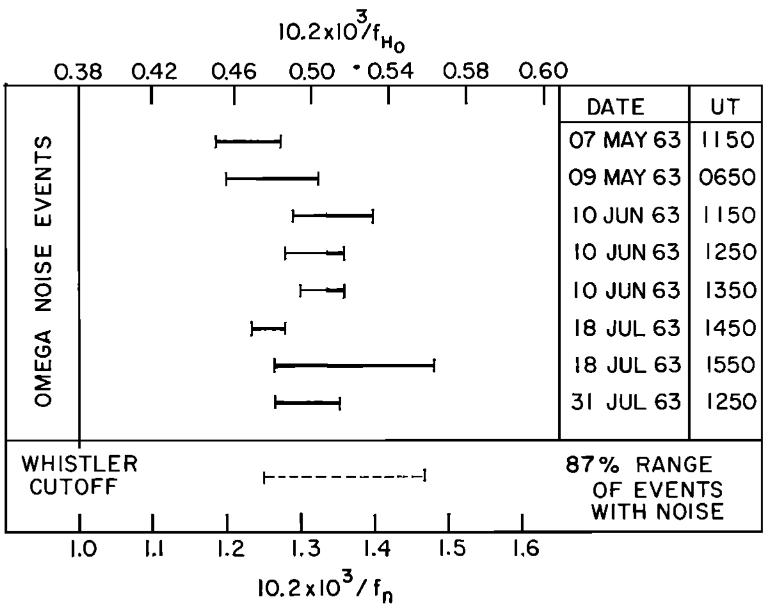

Fig. 9. Cases of artificial triggering of magnetospheric noise by the 10.2-kHz Omega transmitter, showing the estimated range of the ratio of $10.2 \times 10^3/f_n$, where f_n represents the nose frequency (in Hz) of a concurrent natural whistler component with travel time at 10.2 kHz equal to that of an Omega pulse. At the top is a corresponding scale (see text) for the ratio $10.2 \times 10^3/f_{H_0}$, where f_{H_0} is the minimum gyrofrequency along the field-aligned path. The dashed flag below represents the distribution of whistler cutoff data labeled 'with noise' in Figure 3. For these data the lower and upper scales should be considered to represent f_{co}/f_n and f_{co}/f_{H_0}, respectively.

the 0.4–0.5 f_{H_0} range, although there is an apparent preference for the 0.5 f_{H_0} condition. In Figure 5 (Plate 2) upper panel, an analysis similar to that of Figure 8 shows that NAA triggering at 14.7 kHz occurs at about the 0.5 f_{H_0} level. In the case shown in Figure 8, NAA does not trigger, probably owing in part to the absence of a whistler path with suitable cutoff frequency. Weak whistler-mode signals from NAA appear at EI with the stronger subionospheric signal, but these weak signals probably traveled on a path with f_{H_0} well above twice the NAA frequency.

Amplitude Analysis Showing Spectral Details near 0.5 f_{H_0}

The ampligram technique illustrated in Figure 10 was used to obtain crude quantitative information on wave intensity near the cutoff. The coordinates are frequency versus time, with intensity information obtained by a horizontal deflection of the oscilloscope trace instead of intensity modulation of the z axis. The sweeps are 1/75 sec apart, instead of the usual 1/150-sec separation. The 5-kHz calibration represents a nominal signal intensity of 810 μv/m at the loop antenna. The example shows the upper part of a whistler rising to a limiting 'cutoff' frequency at ~7.7 kHz (indicated as $t - t_{co} = 0$), and being followed by a gradually descending noise tone. In this initial study, the horizontal deflections near the cutoff were scaled and compared with the calibration value. Attention was restricted to the vicinity of the cutoff to minimize interpretive problems associated with the Rayspan response to gliding tones.

Some details of whistler intensity versus normalized frequency f/f_{H_0} are shown in Figure 11. The upper group illustrates cases of repeated propagation on a single path within a 2-minute run; the lower group illustrates cases from different runs and a range of paths ~4–5 R_E. The dashed lines carrying below the ampligram background level simply indicate an end to detectable ('smoothly' rising) whistler signals (cf. Figure 10 near $t - t_{co} = 0$). The dashed line connecting points in case F indicates a noisy rising tone with a whistler-like appearance on the record.

Figure 11 illustrates similar cutoff effects in whistlers with widely different maximum intensities and different path equatorial radii. An intensity maximum near the cutoff is indicated in several cases, particularly B, C, E, and G. The cutoff usually involves the disappearance of a detectable rising tone within less than ~13 msec. Note (top of Figure 11) that whistlers propagating on the same path within a 2-minute interval may exhibit cutoff frequencies differing by several hundred cycles.

Details within less than 100 msec of the cutoff time are shown in Figure 12, which displays amplitude (left) and frequency (right) versus

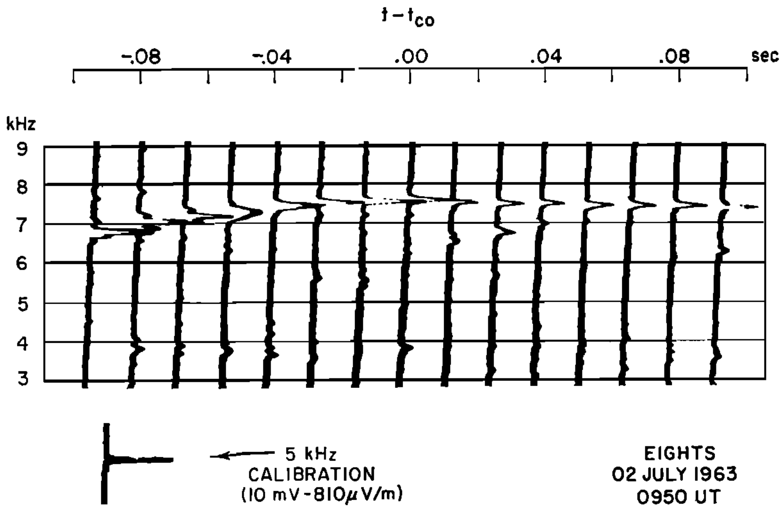

Fig. 10. Sample amplitude display, showing the cutoff of a whistler and beginning of a triggered noise. Rayspan frequency sweeps repeat every 1/75 sec. Time is arbitrarily referred to t_{co}, when the last evidence of a 'smoothly' rising tone is detected.

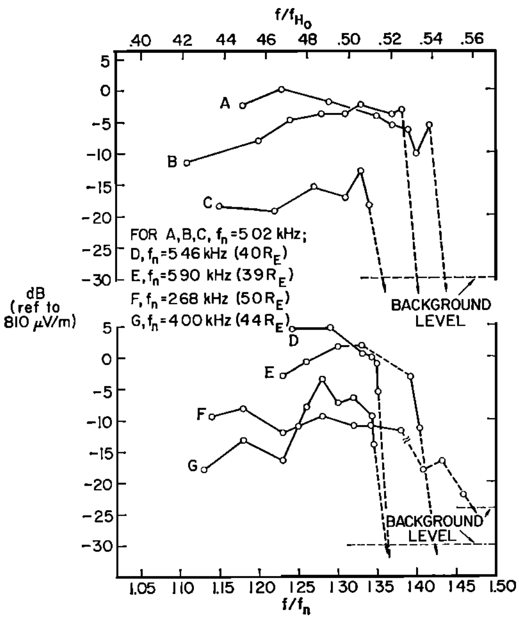

Fig. 11. Some details of whistler intensity versus normalized frequency f/f_{H_0}. Relative variations within events and as between events are to be emphasized; the absolute intensities shown by the db scale require verification by a more refined analysis.

time referred to the time of the cutoff. The flags indicate the half-power bandwidth of the ampligram deflection, typically ~100 cps. Events (*a*) through (*e*) show only a whistler and the first ~30 msec of a triggered noise, whereas (*f*) is a case in which the whistler continues at a lower intensity for ~30 msec after the noise begins.

By extrapolation beyond $t = t_{co}$ of the rising part of the frequency-time curves (*a*) through (*e*) (Figure 12, right), it may be estimated that the intensity of the rising whistler tone drops from its value at $t = t_{co}$ to below the threshold of detectability within a frequency interval of less than 50 cycles. In several cases, notably (*b*), (*d*), and (*e*), there is an anomalous decrease in slope just before the cutoff. Also in several cases, a decrease in whistler intensity begins 10–30 msec before t_{co} and continues until the first sample of the noise tone. The anomalous dispersion may be a spurious effect, but the behavior of case (*e*) suggests that it is real, possibly associated with the mechanism of the triggered noise tone.

Partial Summary of Properties of Noise Triggered by Whistlers

From ampligram analyses of about 20 examples, supplemented by visual examination of thousands of spectra, several points may be made concerning triggered noise of the kind illustrated in Figures 1 and 5 (lower panel).

1. Noise triggered at or near the whistler cutoff is the most frequently observed form of stimulated noise observed at Eights Station (paths observed at Eights usually have equatorial radii in the range 2.5–6 R_E).

2. The noise activity may be similar on paths extending over a range of equatorial radii of 0.5 R_E or greater, or it may be limited to a single active path as in Figure 1*a*. In the case of many active paths the triggered noises are often of similar duration and slope, as in Figures 1*c*, 1*d*, and 5 (lower panel).

3. The intensity of the stimulated noise just after the cutoff is frequently comparable to that of the whistler just before the cutoff. The decreases shown in Figure 12 (left) are small compared with the absolute levels involved.

4. Duration of triggered noises may be from a few msec to several seconds.

5. A triggered noise event frequently involves the following sequence: an initial slight increase

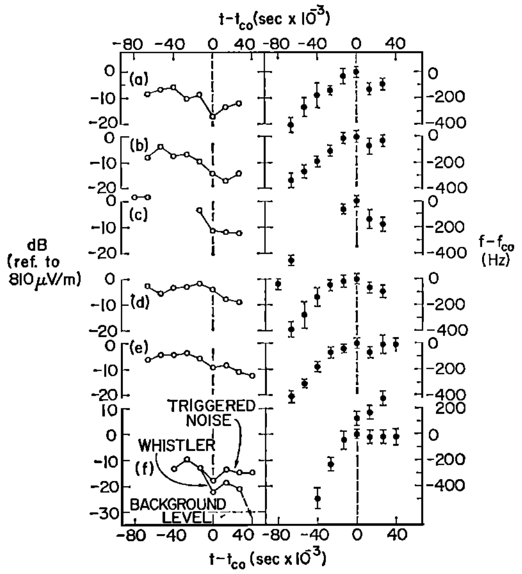

Fig. 12. Some details of the amplitude and frequency-time characteristics of whistlers and triggered noise near the upper cutoff frequency.

in whistler dispersion (cf. Figure 12, case (*f*) on right); the whistler cutoff; a noise tone initially decreasing in frequency with time but often rising later to frequencies above f_{co}; noise tone intensity initially several db below the whistler maximum but later rising to values near or possibly greater than the whistler maximum; noise bandwidth $\leq$100 cps and relatively steady; abrupt termination, sometimes involving a decrease of the order of 20 db within less than 40 msec. (This is only a partial description; many variations in matters of detail are observed.)

6. There is no apparent cutoff effect in the stimulated noise. Once a noise is triggered, its intensity is not affected as its frequency-time curve moves upward through the 0.5 f_{H_0} condition. Maximum intensity in the noise may occur at, say, 0.6 f_{H_0}.

7. Dispersive whistler-mode echoing is not usually observed above f_{co}. A triggered noise rising above f_{co} will usually not exhibit such echoing, although the triggering whistler, on the same path, may do so below f_{co}.

The Intensity Cutoff outside the Plasmasphere

Cutoff and wave growth effects in the tenuous outer region are broadly similar to their counterparts in the plasmasphere. This is suggested in Figure 5, lower panel, by the series of well-defined traces with nose frequency 3–4 kHz and associated paths well outside the plasmapause. For such events, the values of the ratio f_{co}/f_n tend to remain close to an average, but the average is typically lower and more variable from period to period than in the plasmasphere. The tendency toward lower values of f_{co}/f_n is consistent with both (1) *Angerami*'s [1966] findings of a more rapidly varying field-line model of ionization in the plasma trough (see also *Angerami and Carpenter* [1966]), and (2) *Bennett*'s [1965] observation that Smith's condition for untrapping occurs slightly below 0.5 f_H when the ratio of plasma to gyrofrequency becomes sufficiently small. Further study of the nature of magnetospheric ducting at VLF may render possible the use of f_{co} measurements to investigate temporal variations in the field-line distribution of thermal ionization in the plasma trough.

An exception to the usual cutoff behavior occurs at or near the outer surface of the plasmapause. Whistler components propagating to ground stations 'along' this outer surface usually decay gradually in intensity, reaching the background level at frequencies ranging well above and below 0.5 f_{H_0}.

Other Types of Upper Cutoff

The two most commonly observed upper cutoff effects in whistlers are: (1) the cutoff (described in this paper) that occurs *above* the nose frequency and at a fixed value of *normalized* frequency $f/f_{H_0} = 0.5$; (2) the cutoff that usually occurs *below* the nose frequency and at a fixed *absolute* level of frequency in the range ~10–15 kHz. The former is found most frequently on paths with radii greater than 3.5 R_E, the latter on paths with radii less than 3.5 R_E ($f_n > 8$ kHz). The second class involves a comparatively gradual decay in intensity and is not usually associated with noise. It is a type of cutoff familiar to whistler workers, since the location of most IGY whistler recorders favored the observation of paths with relatively high nose frequencies.

Cutoffs below the nose frequency in the range 10–15 kHz may possibly be attributed to a corresponding dropoff in the amplitude spectrum of whistler-producing lightning sources [*Helliwell et al*, 1958]. This hypothesis is supported by observations of simultaneous propagation on a magnetospheric path with equatorial radius ~3 R_E of: (1) whistlers with intensity cutoffs below 15 kHz and (2) Morse-code transmissions at about 18 kHz from fixed-frequency VLF transmitters (J. Katsufrakis, personal communication). The frequently large signal-to-noise ratio of the code receptions suggests that the low whistler intensity at 18 kHz is primarily a source effect.

Cyclotron resonance interactions may play a role in the cutoffs below the nose frequency just described, but this role will be difficult to appraise until the effects of the amplitude spectrum are properly identified.

Comments on the Field-Line Model of Thermal Ionization used in Calculating f_{co}/f_{H_0}

In this research, the ratio of the observables f_{co}/f_n was found to be roughly constant at 1.3. The value of the corresponding ratio $f_{co}/f_H \sim 0.5$ was determined using the relation $f_n = 0.38\, f_{H_0}$, which is an approximation to some calculations of the ratio f_n/f_{H_0} carried out by *Angerami* [1966]. Angerami's calculations involved use of a diffusive-equilibrium model of the distribution of ionization along the field lines. He demonstrated experimentally that this model is usually appropriate for describing the plasmasphere and recently obtained independent support for his conclusions from a study of ducted whistlers on OGO 1 [*Smith and Angerami*, 1968]. The present study supports Angerami's findings, in that by employing a relation between f_n and f_{H_0} based on the diffusive-equilibrium model, the whistler intensity cutoff is found to occur within a narrow range around 0.5 f_{H_0}, as predicted by Smith's ray theory of trapping in ducts. If a more rapidly varying model such as $N \propto R^{-4}$ were used, the data on f_{co}/f_{H_0} would be concentrated at some level near 0.6 f_{H_0}, a condition for which there is no theoretical support.

Conclusions

Magnetospheric whistlers propagating within the plasmasphere on paths with equatorial radii $> 3.5 R_E$ typically exhibit an abrupt upper cutoff in intensity above the nose frequency. In 541 measured cases, mostly recorded at Eights, Antarctica ($L \sim 4$), the ratio of the observables f_{co}/f_n was 1.33 $\pm$ 0.08 (70% range). Using the empirically supported diffusive-equilibrium model of the distribution of thermal electrons in the plasmasphere, the calculated value of the ratio of cutoff to minimum path gyrofrequency f_{co}/f_{H_0} is 0.51 $\pm$ 0.03.

A number of attempts have been made to explain the upper cutoff of whistlers in terms of a cyclotron resonance interaction [e.g., *Liemohn*, 1967]. However, the invariance of the ratio of the observables f_{co}/f_n with respect to path equatorial radius, local time, and magnetic activity suggests that the frequency of the cutoff is controlled by some kind of propagation effect and not by the details of the resonant particle distribution. To control the cutoff frequency, the latter would be subject to severe and probably unrealistic constraints. Since the numerical value of the derived ratio f_{co}/f_{H_0} is $\sim$0.5, it is suggested that the propagation effect involved is the half-gyrofrequency ducting effect predicted by *Smith* [1961], using ray theory for propagation in tubes of enhanced ionization. According to the theory, a ray trapped in a duct will be untrapped beyond a point at which its frequency is half the local gyrofrequency.

Wave-particle interactions must certainly be invoked to explain the details of the amplitude spectrum near the cutoff, and it is likely that a general theory of the cutoff will require consideration of both ducting and wave growth.

In the present work, several particular features of wave growth have been identified, including a peak in whistler intensity that frequently appears in the range 0.4–0.5 f_{H_0}. This intensity peak is evidenced on spectrographic records by the band-selective behavior of discrete periodic emissions, the amplitude spectra of whistlers propagating from many faint sources on an 'unusual' duct, and in particular the stimulation of noise at $\sim$0.5 f_{H_0} by both whistlers and a low power ($\sim$100 watts) controlled source.

A crude amplitude analysis shows the whistler cutoff to involve an intensity decrease of the order of 20 db within a time interval $\Delta t < 13$ msec and a frequency interval $\Delta f < 50$ Hz. The cutoff may vary from case to case in matters of fine detail, both within a given 2-minute run and as between runs, but the general form of the amplitude spectrum is independent of path equatorial radius and of whistler intensity.

Acknowledgments. The quality and extent of information on the magnetosphere obtainable from whistlers recorded at Eights, Antarctica, defies credulity. I (once again) congratulate the Office of Antarctic Programs of the National Science Foundation and the U. S. Navy Antarctic Support Force for establishing and supporting Eights Station, and also congratulate J. Katsufrakis, supervisor of Stanford University VLF field activities in the Antarctic, and M. Trimpi, 1963 field engineer at Eights.

This research was initiated as the result of conversations with H. B. Liemohn and F. L. Scarf. I have benefited from discussions with R. A. Helliwell, R. L. Smith, T. S. Jørgensen, T. F. Bell, I. Kimura, and S. M. Bennett. I am indebted to M. Trimpi for preparing the ampligrams and to R. White, B. G. Lee, and K. Stone for assistance in data reduction.

This research was supported in part by the Office of Antarctic Programs and the Atmospheric Sciences Section of the National Science Foundation and in part by the U. S. Air Force, Office of Scientific Research of the Office of Aerospace Research.

References

Angerami, J. J., A whistler study of the distribution of thermal electrons in the magnetosphere, Ph.D. thesis, *Tech. Rept. 3412-7,* Radioscience Lab., Stanford Electronics Labs., Stanford University, Stanford, Calif., May 1966.

Angerami, J. J., and D. L. Carpenter, Whistler studies of the plasmapause in the magnetosphere, 2, Electron density and total tube content near the knee in magnetospheric ionization, *J. Geophys. Res., 71,* 711, 1966.

Bennett, S. M., An improved whistler-mode refractive index equation, *J. Geophys. Res., 70,* 725, 1965.

Brice, Neil, Multiphase periodic very-low-frequency emissions, *Radio Sci., 69D,* 257, 1965.

Eviatar, A., A. M. Lenchek, and S. F. Singer, Distribution of density in an ion-exosphere of a nonrotating planet, *Phys. Fluids, 7,* 1775, 1964.

Guthart, H., An anisotropic electron velocity distribution for the cyclotron absorption of whistlers and VLF emissions, *Radio Sci., 69D,* 1403, 1965*a*.

Guthart, H., Nose whistler dispersion as a measure of magnetosphere electron temperature, *Radio Sci., 69D,* 1417, 1965*b*.

Helliwell, R. A., *Whistlers and Related Ionospheric Phenomena,* Stanford University Press, Stanford, Calif., 1965.

Helliwell, R. A., A. G. Jean, and W. L. Taylor, Some properties of lightning impulses which produce whistlers, *Proc. IRE, 46,* 1760, October 1958.

Helliwell, R. A., J. Katsufrakis, M. Trimpi, and N. Brice, Artificially stimulated very-low-frequency radiation from the ionosphere, *J. Geophys. Res., 69,* 2391, 1964.

Kimura, I., Triggering of VLF magnetospheric noise by a low power (~100 watts) transmitter, *J. Geophys. Res., 73,* 445, 1968.

Laaspere, T., M. G. Morgan, and W. C. Johnson, Some results of five years of whistler observations from Labrador to Antarctica, *Proc. IEEE, 51,* 554, 1963.

Laaspere, T., M. G. Morgan, and W. C. Johnson, Chorus, hiss, and other audio-frequency emissions at stations of the whistlers-east network, *Proc. IEEE, 52,* 1331, 1964.

Liemohn, H. B., Cyclotron-resonance amplification of VLF and ULF whistlers, *J. Geophys. Res., 72,* 39, 1967.

Liemohn, H. B., and F. L. Scarf, Exospheric electron temperatures from nose whistler attenuation, *J. Geophys. Res., 67,* 1785, 1962*a*.

Liemohn, H. B., and F. L. Scarf, Whistler attenuation by electrons with an $E^{-2.5}$ distribution, *J. Geophys. Res., 67,* 4163, 1962*b*.

Liemohn, H. B., and F. L. Scarf, Whistler determination of electron energy and density distributions in the magnetosphere, *J. Geophys. Res., 69,* 883, 1964.

Scarf, F. L., Landau damping and the attenuation of whistlers, *Phys. Fluids, 5,* 6, 1962.

Smith, R. L., Propagation characteristics of whistlers trapped in field-aligned columns of enhanced ionization, *J. Geophys. Res., 66,* 3699, 1961.

Smith, R. L., and J. J. Angerami, Magnetospheric properties deduced from OGO 1 observations of ducted and nonducted whistlers, *J. Geophys. Res., 73,* 1, 1968.

(Received October 12, 1967.)